Thematic Mapper Research in the Earth Sciences

Title of the Project:

Small Scale Patches of Suspended Matter and Phytoplankton in the Elbe River Estuary, German Bight and Tidal Flats

– Progress Report –

Principal investigator: H. Grassl
Responsible scientists: R. Doerffer, J. Fischer,
C. Brockmann and M. Stössel

GKSS Forschungszentrum Geesthacht
FRG

October 9, 1987

Contents

Chapter 1

Introduction

1.1 The Scientific Problem

The coastal region of the German Bight is characterized - as other areas of the North Sea - by a complicated distribution of different water masses containing high concentration of various substances, particulary suspended matter and phytoplankton . These two concentration parameters are of high importance in ecological studies: Suspended matter has to be regarded as the main carrier of various inorganic and organic substances including pollutants and as the main substrate for biochemical processes. The phytoplankton distribution indicates areas of high biological activity (production, grazing, remineralisation etc.).

Present techniques to investigate or monitor coastal water masses of the North Sea are insufficient, because they can provide only a raw idea about the gross mass of substances involved in ecological processes, their distribution dynamics and the transport mechanisms of the solid water constituents. Previous investigations indicate that transport and ecological processes -as phytoplankton growth - are linked to small scale hydrographic features namely local fronts, eddies , convergence zones and areas of high turbulence. As main parameters, which control the formation of these features, one has to consider the shallow water bottom topography, the complex topography and current regime of the wadden sea, the fresh water run-off of the Elbe and Weser estuaries, the tidal currents and the general circulation of the North Sea.

Aicraft data show that small scale temperature fronts and convergence zones may occur with sizes smaller than the geometric resolution of NOAA and CZCS data. These data indicate also that smallscale structures are important for the transport of solid matter, which is characterized by continuous sedimentation and resuspension, as well as for the occurrence of high plankton concentrations.

It is obvious that the small scale distribution patterns require much more attention. Its investigation is an important prerequisite for the understanding of the ecological process in this type of coastal zone.

The combination of high geometric resolution along with the spectral capability of the Thematic Mapper provides the unique opportunity to get a much better insight into this complex marine system and to improve the strategy for environmental monitoring programmes.

1.2 Experimental Objectives

At the beginning of this TM research projects the following objectives were formulated:

The overall goal is to understand the mechanisms leading to the complex distribution patterns in a shallow coastal region, which is influenced by an estuary.

Special hypotheses are:

- Bottom topography and wind field control the tide depending formation of small scale water bodies, eddies and fronts.
- The sediment transport mechanism is based on multiple resuspension and sedimentation events, which happen on small scales as a function of areas with variable turbulence mainly driven by the tidal currents.
- High phytoplankton concentrations are related to samll scale fronts.

For the application of TM data it will be necessary furthermore to test the following hypotheses:

- The TM allows us to determine at least the concentration of the total suspended matter concentration and to map their horizontal distribution.
- A separation of the contribution of suspended matter and phytoplankton is possible.
- Dynamic processes can be studied by combining TM data, ship data and multiple aerial surveys within short intervals.

1.3 Project Strategy

The strategy of the investigation contains the following elements:

- Model simulation of the TM and response study with respect to quantitive measurements of suspended matter and phytoplankton chlorophyll. This study should lead to an atmospheric correction procedure and to algorithms for deriving the concentration parameters.
- Field experiments with ship and aircraft for ground truth and for analyzing the tide depending dynamics of the distribution phenomena.

- Analysis of TM data with respect to the information content, distribution maps and the relation between the distribution of mainly suspended matter and parameters as bottom topography, the wind field and the current regime.

Chapter 2

The Field Experiment

2.1 Objectives and Strategy

The objective of the field experiment was to collect ground truth data for the calibration of the TM data in terms of radiances and concentration parameters and for the atmospheric correction. Furthermore the ship data should give a link to parameters, which are not directly accessible by radiance measurements; this is particularly the relation between water topography, the actual water depth and the suspended matter distribution at the surface. For this reason we selected sections in the vicinity of the Elbe mouth, where we expected a strong variation in the suspended matter distribution because of a distinct bottom topography. These sections with a length of 10 - 20 km were traced with our research vessel 3 -4 times during a tidal phase. A prerequisite to meet the same sections again and to identify the ship tracks within the satellite image was an accurate navigation. The Syledis navigator equipment allowed us to position the ship with an accuracy of about 1 m. In addition to the profiles time series of the same parameters were recorded during anchor stations. In addition a research aircraft of the DFVLR was operating the Daedalus Thematic Mapper Simulator at some days of the Experiment.

2.2 Methodology of the Experiment

The experiment was carried out during the period May 1st - May 17th 1986. The area and the profiles shows Fig. 2.1 .TM overflights were expected for the 1, 8 and 17 of May. During this time a total number of 29 horizontal profiles were recorded with the following instrumentation:

- water was continuously pumped from about 1.5 m depth through a ME-TRAWATT turbidity meter, an AMINCO fluorometer for chlorophyll concentration and a ME cell to measure temperature and salinity.

- a SUAREZ in situ scatterometer was used to determine the time lag between the in situ turbidity and the response of the turbidity meter in the flow cuvette.
- The water leaving radiance was measured with a DFVLR 12 channel filtherwheel spectrometer continuously from the bow of the ship with a resloution of 2 spectra per second. This high rate was necessary to allow integration with a clearance procedure to achieve the 10 m resolution of the other instruments.
- An irradiance meter mounted at the top of the ship was used to record the downwelling global radiation.
- The actual water depth was measured with an ATLAS echosounder.

All data including radiance spectra, turbidity, downwelling irradiance, water temperature, salinity and water depth were stored together with time and position in the central computer every ten meters during cruising and every minute during anchor position.

For calibrating the instruments water samples were taken whenever strong changes in concentrations were observed on the plotter. These water samples were analyzed for:

- suspended matter dry weight
- aborption of the filtrate at 380 and 420 nm wavelength to determine the Gelbstoff concentration
- chlorophyll and phaeophytin concentration
- conductivity at a temperature of 20° C.

All ship data and the values of the laboratory analysis were given to a BULL SPS 9 UNIX computer for further analysis .

2.3 Results

The shipborne data have been analyzed up to now with respect to the following questions:

- relation between turbidity and total suspended matter dry weight,
- typical scales in the variation of turbidity,
- cross correlation between turbidity and water depth.

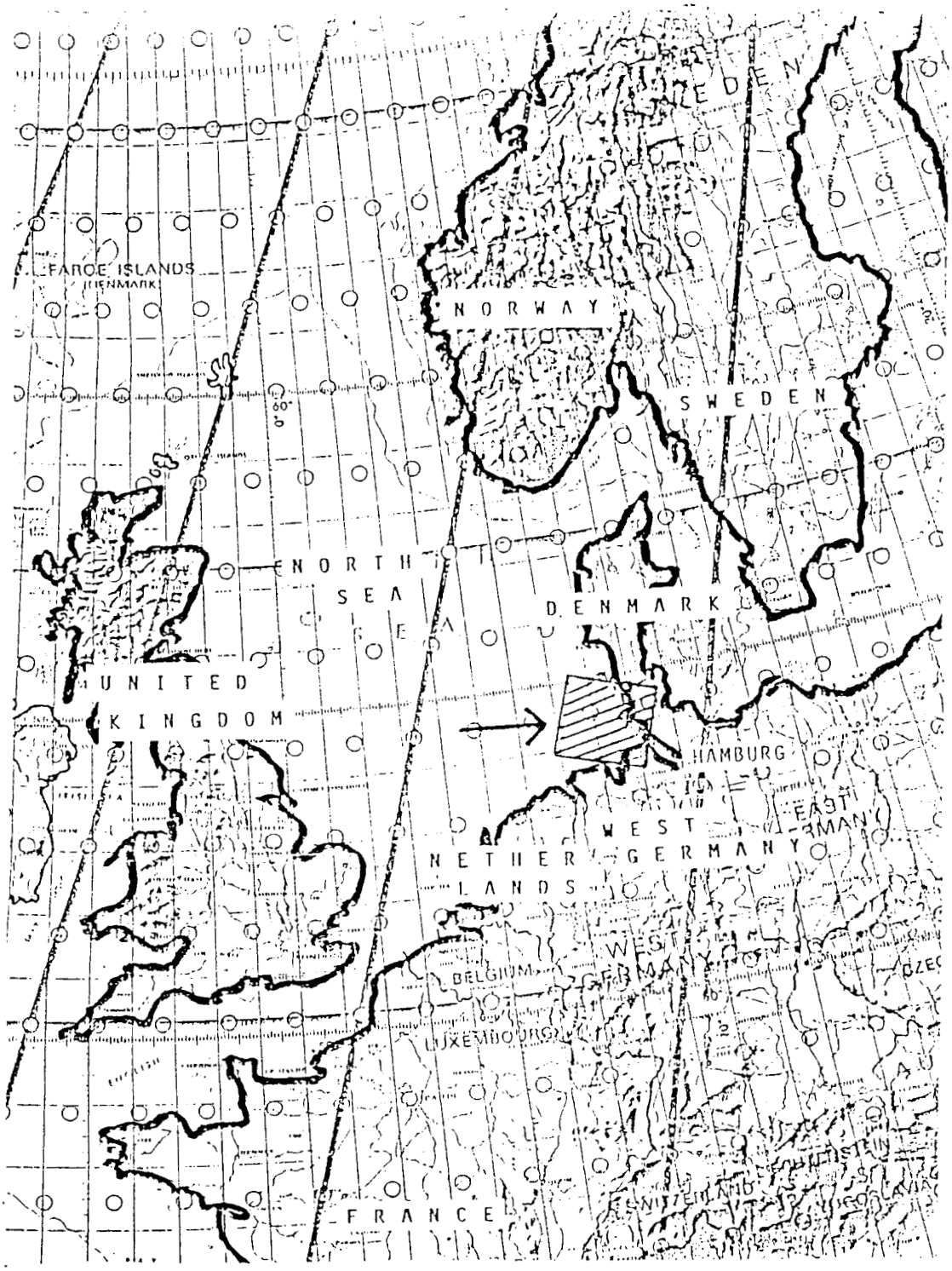

Figure 2.1: Location of the research aerea.

The relation between the turbidity, measured by the METRAWATT continuous flow instrument, and the total suspended matter dry weight shows a high linear regression with a confidence level > 99% (Fig. 2.2). This excellent relationship was surprising, because we normally find within the area a strong variation of particle sizes and composition.

A typical horizontal suspended matter profile of 15 km length together with the depth profile is presented in Fig. 2.3. It demonstrates the high concentration and variability of suspended matter in the coastal zone which is characterized by shallow water, strong currents and a complex system of sand banks and tidal flats. The relatively smooth profile indicates that changes in the concentration happen on a scale of 100 to 1 km. At the present state of the evaluation we are not sure if higher frequencies are suppressed by the measuring technique, because visual observations show often smaller patches at specific tidal phases. This question has to be analyzed with the radiance spectra.

The correlation between water depth and suspended matter is shown in Fig. 2.4. This figure confirms our hypothesis, that there exists a general relation between the water depth and the suspended matter concentration at the surface. Two reasons may be responsible for this result: The tidal current and the turbulence become stronger whenever the water has to flow over shallower areas; the vertical turbidity profile decreases from the bottom to the surface.

As the next step we have tried to get information about typical scales by auto- and cross-correlation. The results of this analysis are shown in Fig. 2.5. Indicated are the correlation coefficient as solid line and the 95% confidence levels as dotted lines. The water depth is significantly correlated until scales up to 1.3 km, the suspended matter up to 800 m.

The cross correlation between both parameters confirms the expected significant negative correlation up to a distance of 1.2 km.

The analysis is a confirmation for our hypothesis, that a main factor controlling the horizontal distribution of suspended matter fields is the water depth.

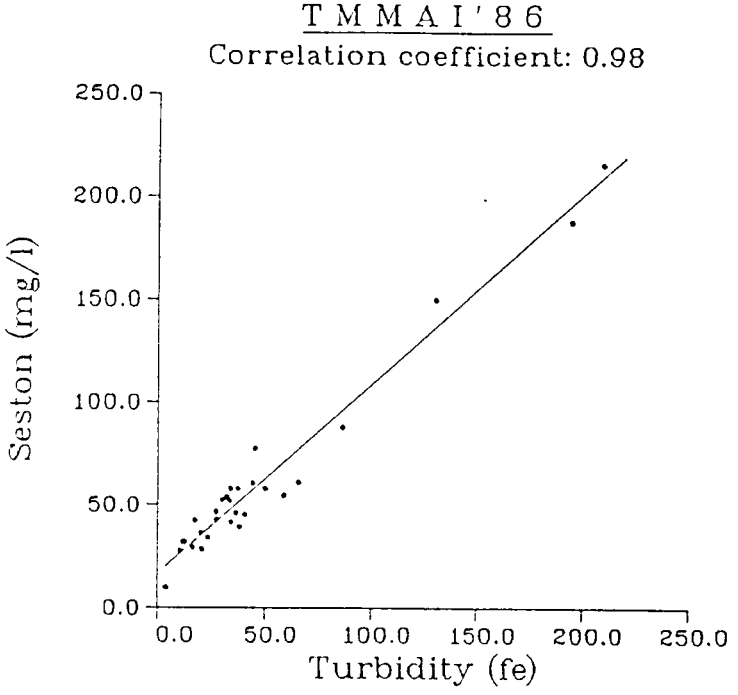

Figure 2.2: Correlation between turbidity measured with the METRAWATT turbidity meter and total suspended matter dry weight as determined from water samples.

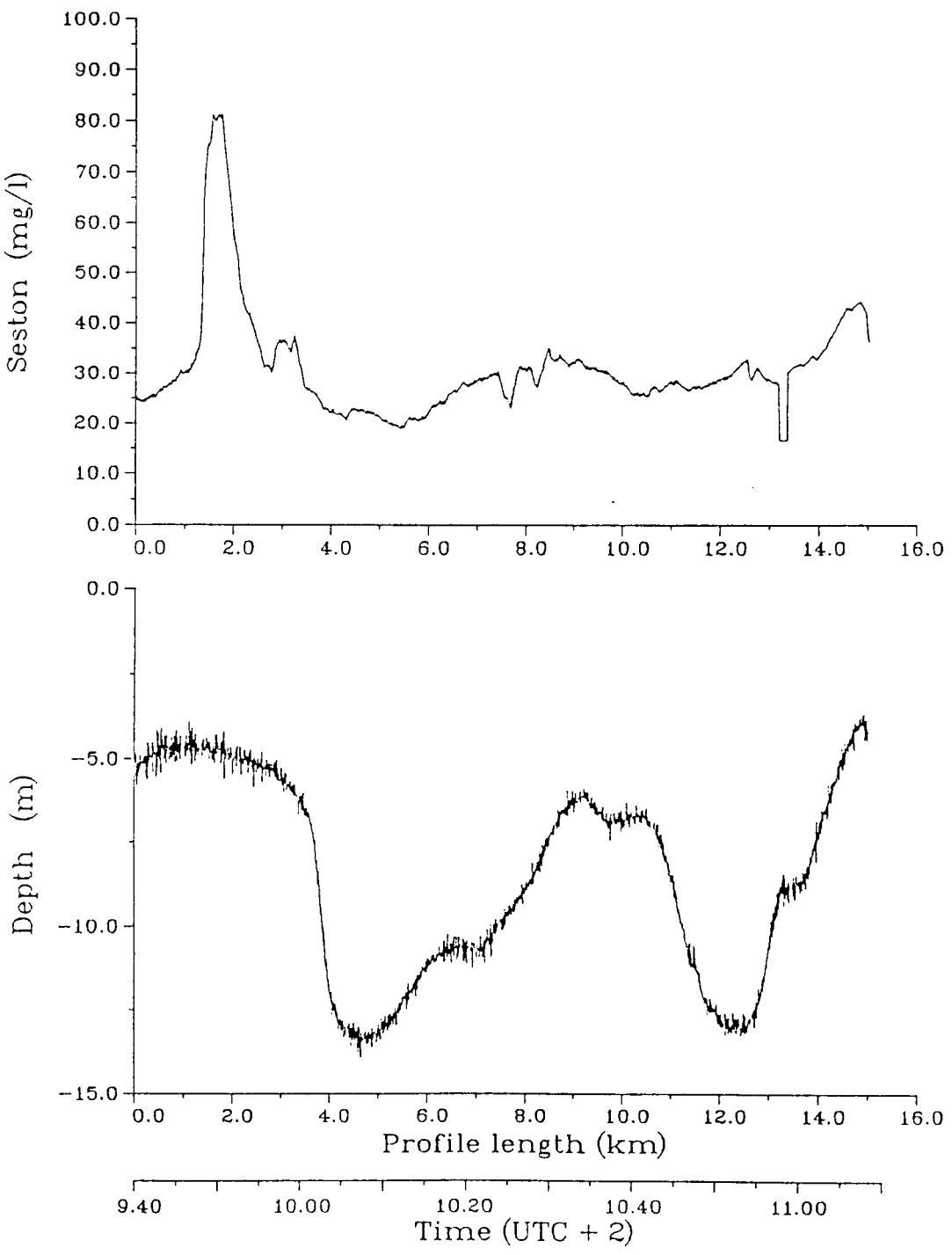

Figure 2.3: Horizontal profile of suspended matter and water depth.

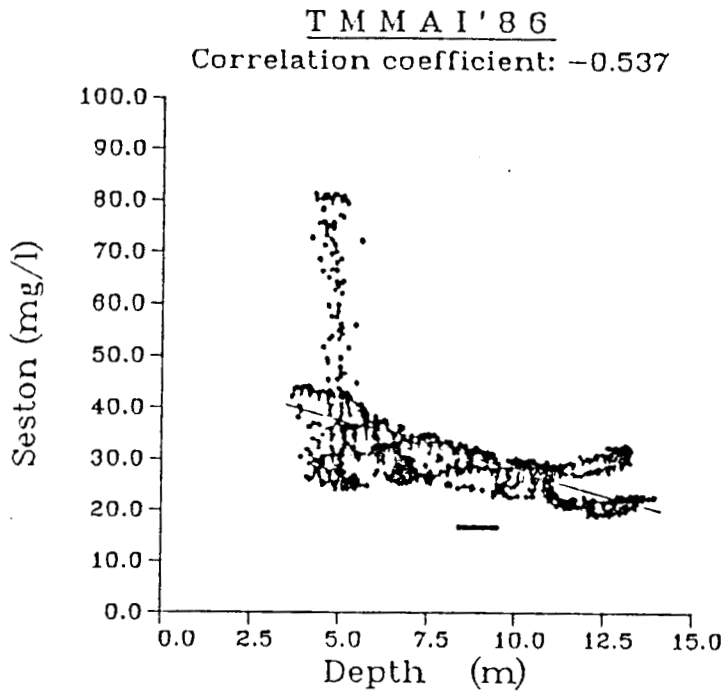

Figure 2.4: Correlation between waterdepth and suspended matter concentration in $\approx$ 1.5 m depth.

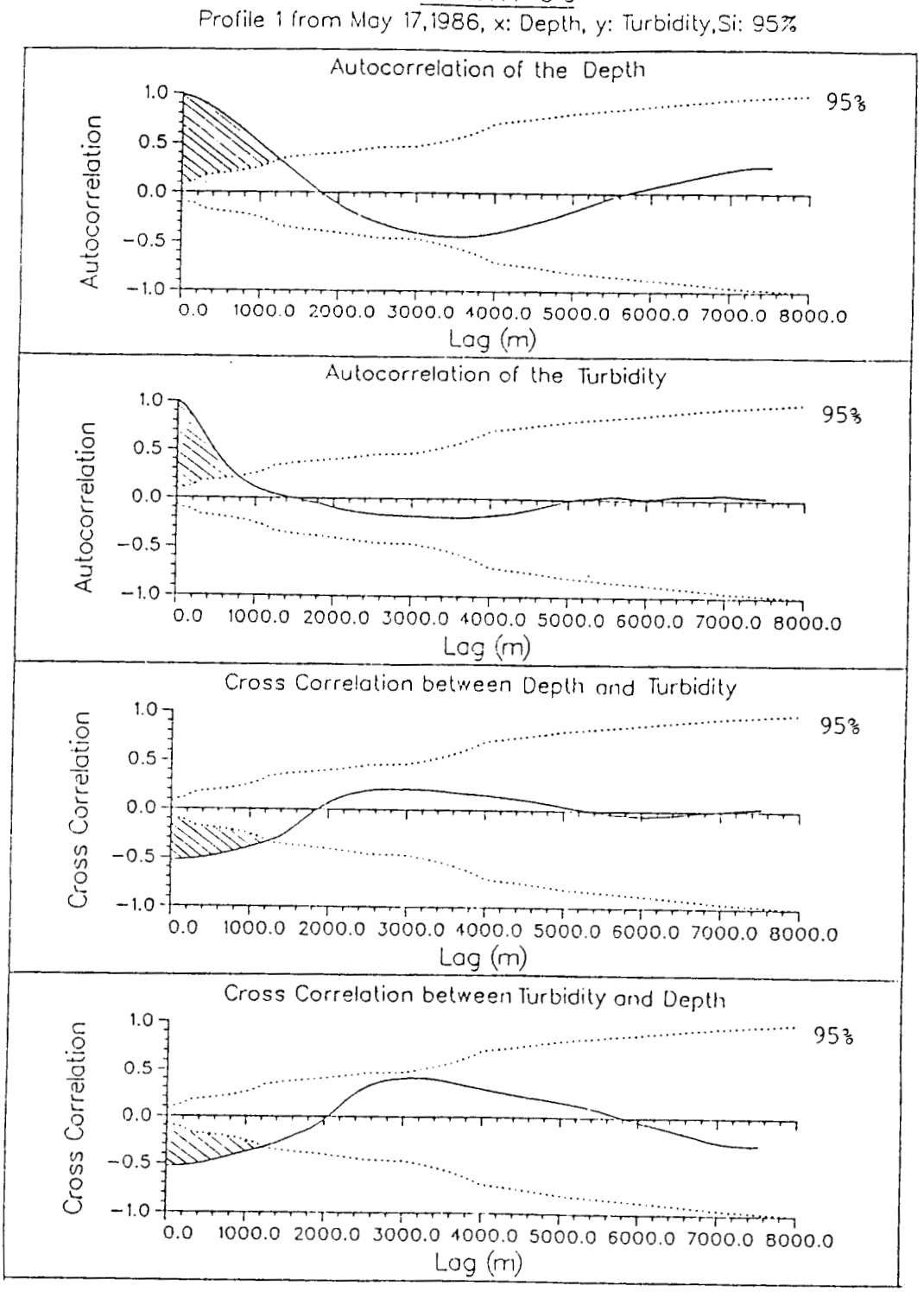

Figure 2.5: Auto correlation of the suspended matter distribution and the water depth and cross-correlation between both parameters of the profile of Fig. 2.3.

Chapter 3

Evaluation of a Thematic Mapper Scene

3.1 Objectives

The initial steps in the analysis of TM data were:

- to analyze the radiometric resolution and signal/noise ratio with respect to our task to derive concentrations of suspended matter and chlorophyll
- to investigate possibilities for atmospheric correction
- to analyze the information content of the TM spectra over turbid water areas.

Further analysis will then deal with the scales and the relation between water depth, the actual current and the suspended matter distribution derived from the TM scenes, the correlation with water mass distribution indicated by the thermal channel and with the information content of dry wadden sea areas.

3.2 Evaluation Procedures

To evaluate the TM scenes we had to develop or adapt the following procedures and computer programs:

- procedure to read the tape and transform the information into our image processing file structure
- procedure to calculate pixel coordinates from geo geographical coordinates in order to identify our ship course in the scene, to plot the ship course into the scence and to pick the pixel values out of the scene and add it into our file with ship data for comparing ship and TM data;

- a classification program, based on a hierachical non supervised automatic classification in order to separate different areas of water, sand banks, tidal flats, land, clouds;
- a factor analysis program which considers areas of only one class in order to estimate the number of parameters (factors) which determine the variations in the TM spectra and calculates the scores for each factor in form of an image.

Other programs have been developed for analyzing the effects of the atmosphere; they are discussed in chapter 4.

For our first analysis we used the TM scene of May 17th, which is nearly cloud-free, with small influence by haze and where we have good ground truth. Furthermore we have analyzed a scene of Aug. 1984 in order to check the radiance dynamics over water and compare it with model calculations.

3.3 Results

Histogramms of all channels calculated only for the water area of the scene (Fig. 3.1) show the low Digital Numbers (DN) and the very narrow ranges. If one calculates the radiances and compares it with corresponding suspended matter concentrations (s.chap.4), it becomes clear, that the signal/noise ratio is not always sufficient for deriving suspended matter concentrations with the required accuracy, although it is possible to derive a distribution map for analyzing scales. For a detailed analysis we have considered the corresponding TM data of our ship profile (discussed in chapter 2). Fig. 3.2 shows the mean values, the standard deviations (hatched) and the overall range of the radiances along the profile. Obvious is the strong influence of the Rayleigh scattering of the atmosphere which is manifested in the steep decrease from blue to red. Along the ship track the variations are rather small compared to the noise (Fig. 3.3). From this plot it is obvious that channel 3 has the best signal/noise ratio with respect to suspended matter variations. Even the near infrared channel 4 is still influenced by the suspended matter scattering, while the blue channel 1 has the lowest variability, because it is dominated by atmospheric scattering. An integration of 5×5 pixels improves the S/N and improves the sturcture in the profile (Fig. 3.4).

Factor analysis (Doerffer,1981) opens the possibility to estimate how many independent factors determine the spectral variability in the data. To apply this method we have first separated the pure water area by a hierachical unsupervised classification procedure (Fig. 3.5). It has been found that channel 4 is sufficient for a clear separation of water surfaces.

The factor analysis was then applied only to those pixels classified as water area. This restriction is necessary, because otherwise cloud and land pixels

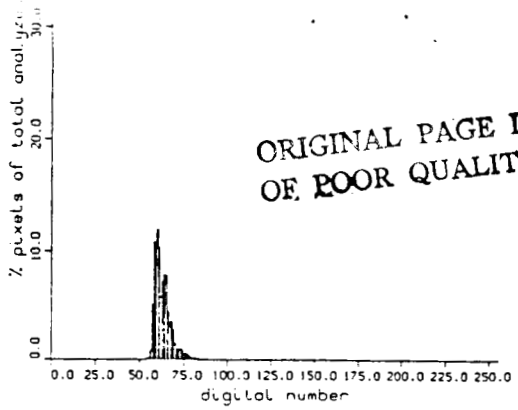

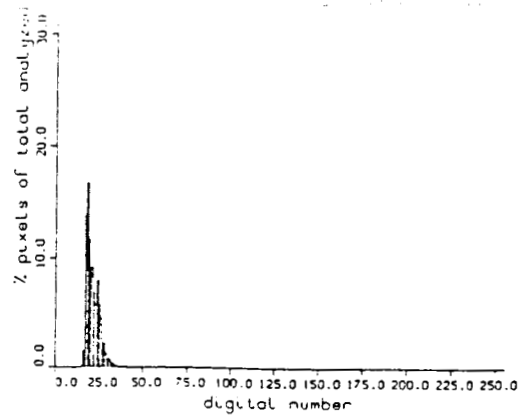

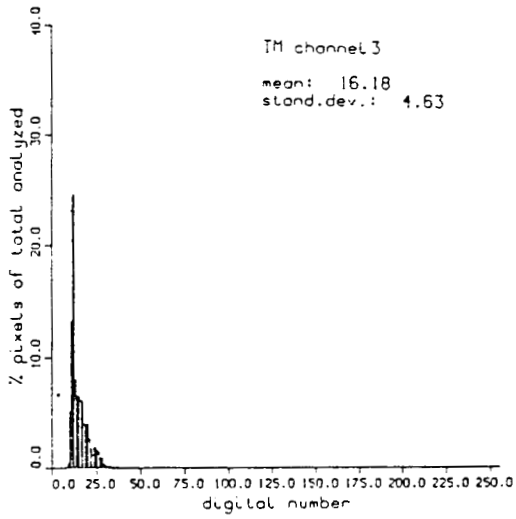

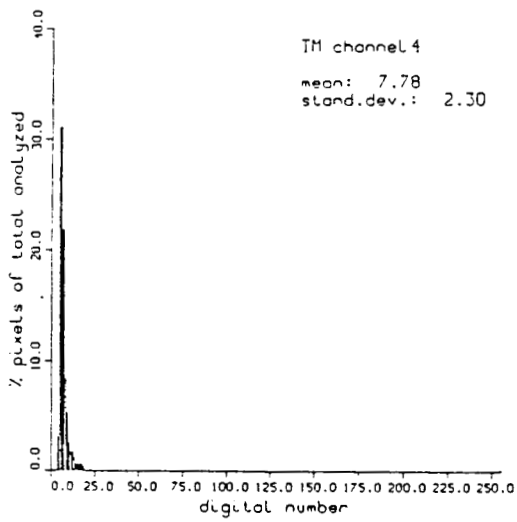

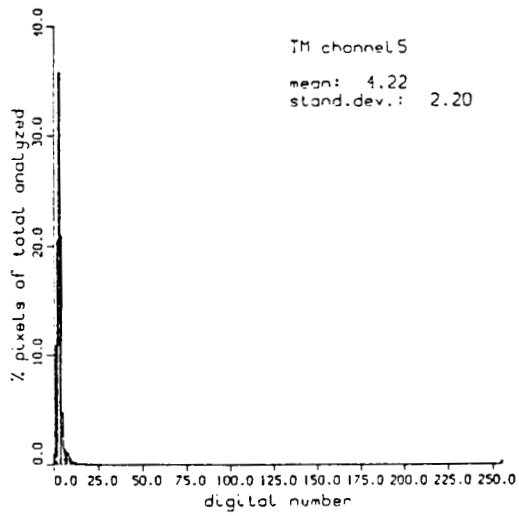

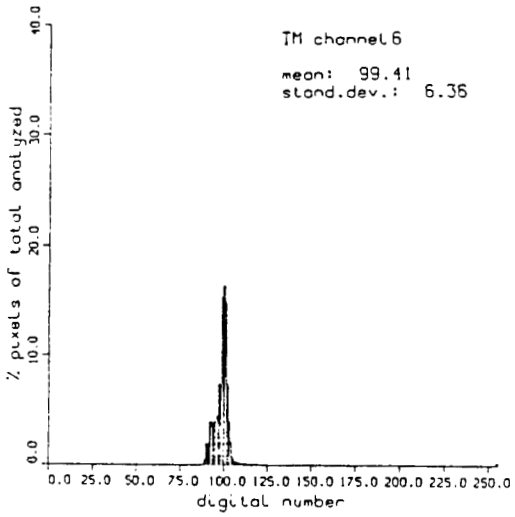

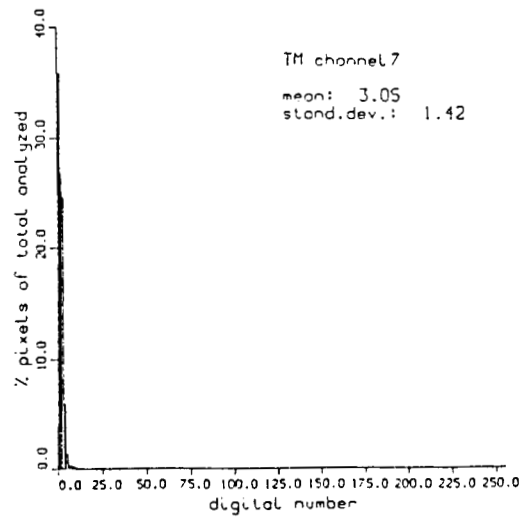

Fig. 3.3.1: Statistical parameters and histograms of all 7 TM channels of only "water pixels".

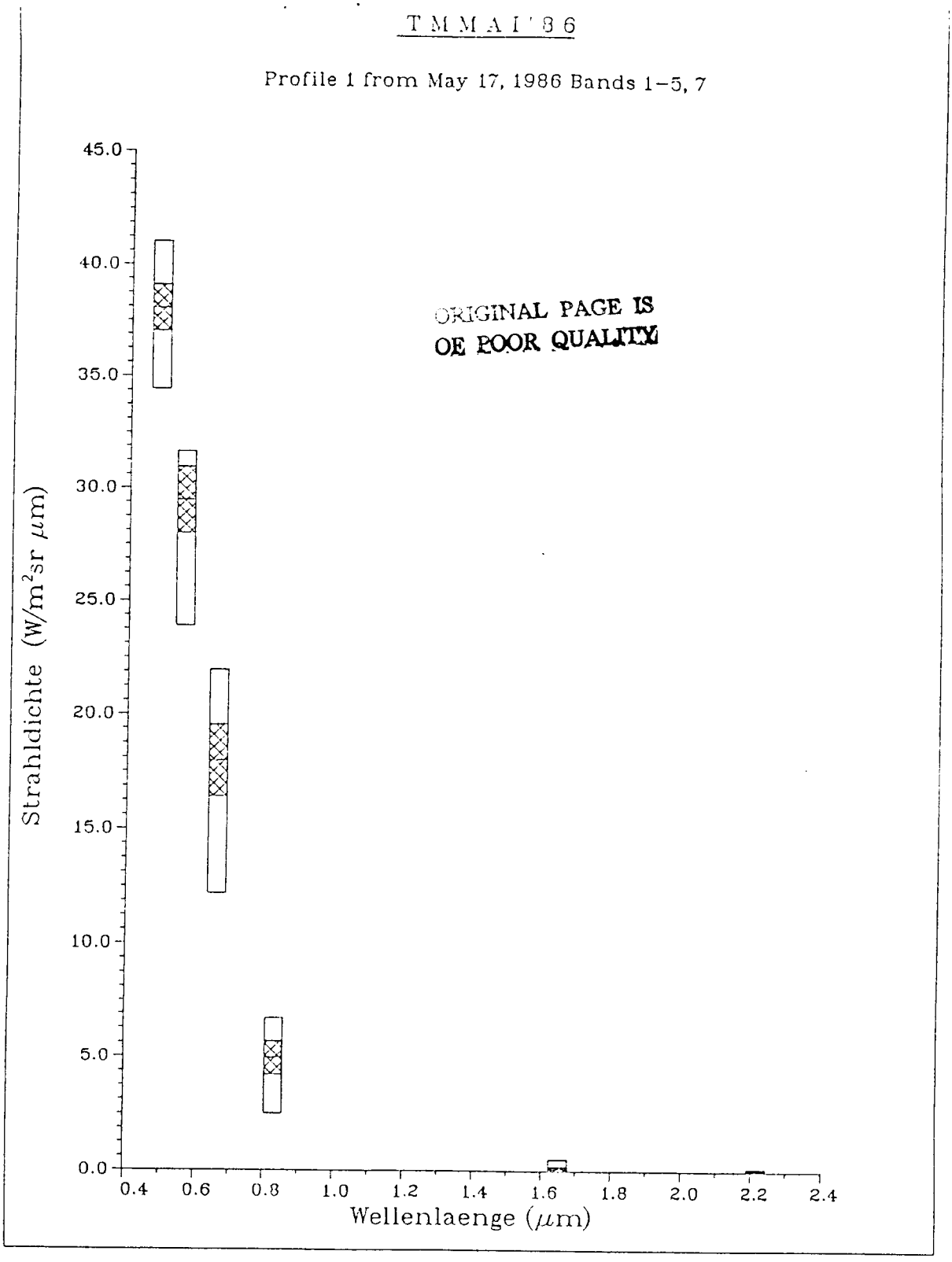

Figure 3.2: The variability of the TM radiances of the profile in Fig. 3.3.

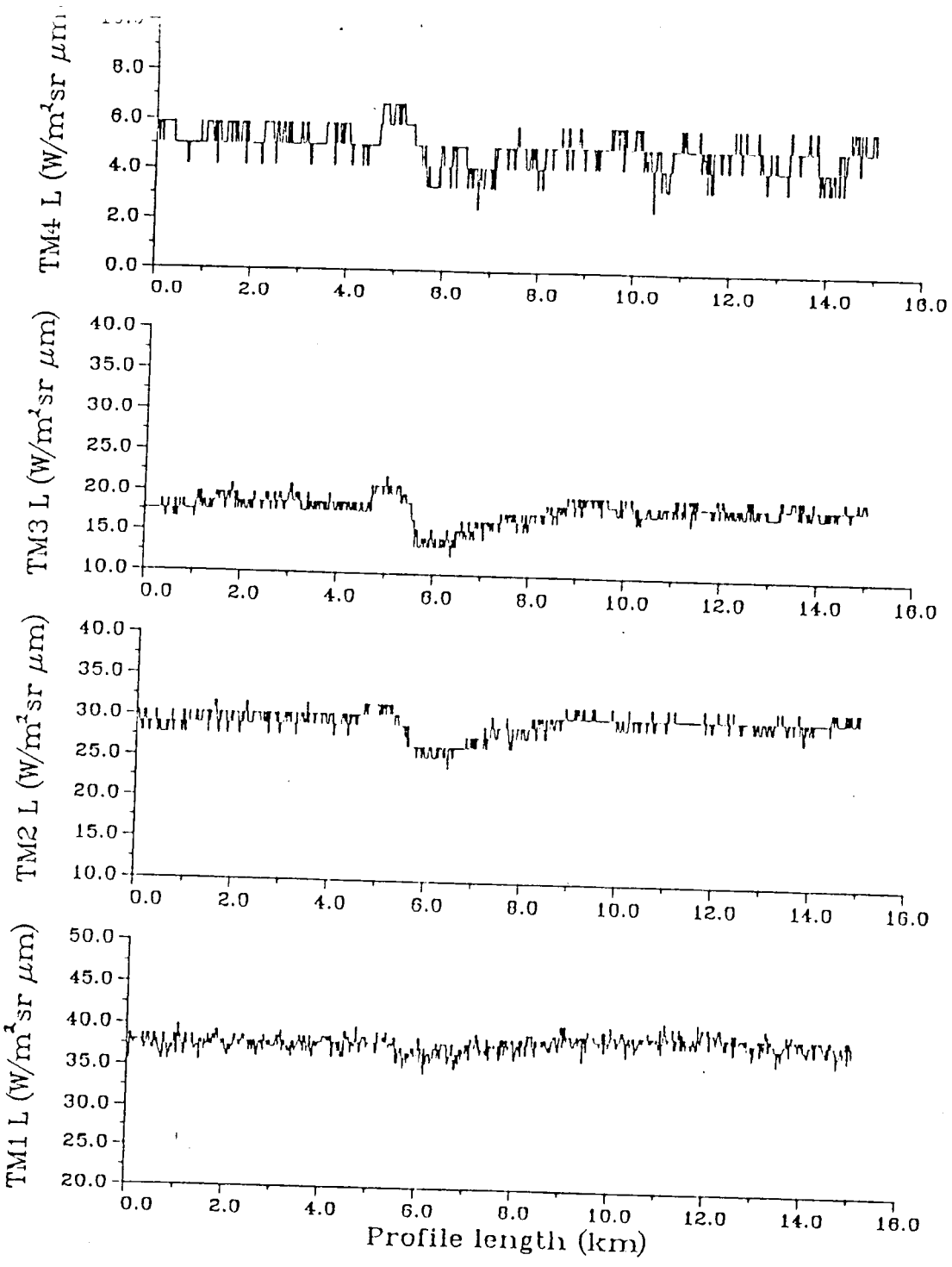

Figure 3.3: Radiances of TM channels 1-4 along the ship track (see Fig. 2.3.

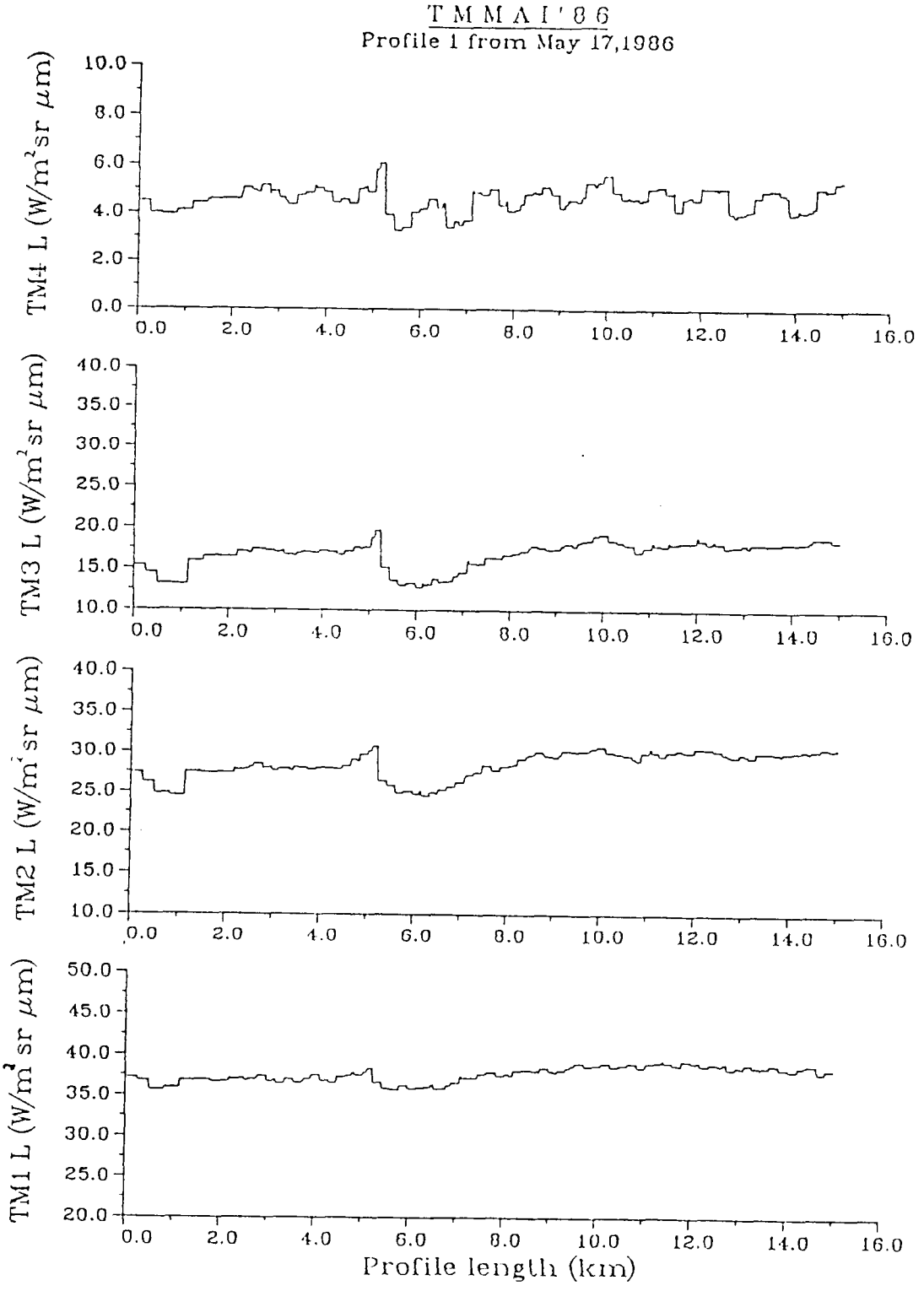

Figure 3.4: Radiances as in Fig. 3.3 after integration of 5 × 5 pixels.

	TM 1	TM 2	TM 3	TM 4	TM 5	TM 6	TM 7	H^2
TM 1	1.000	0.919	0.905	0.821	0.562	0.258	0.426	0.919
TM 2	0.919	1.000	0.962	0.808	0.475	0.338	0.367	0.962
TM 3	0.905	0.962	1.000	0.856	0.384	0.340	0.369	0.962
TM 4	0.821	0.808	0.856	1.000	0.617	0.295	0.468	0.856
TM 5	0.562	0.475	0.484	0.617	1.000	0.174	0.579	0.617
TM 6	0.258	0.338	0.340	0.295	0.174	1.000	0.125	0.340
TM 7	0.426	0.367	0.369	0.468	0.579	0.125	1.000	0.579

Table 3.1: Korrelationmatrix and Kommunalitäten

would change the covariance matrix and thus hide or suppress the variances of the radiances over water.

The resulting correlation matrix is given in table (3.1). This matrix indicates three groups of channels: channels 1-4 are highly correlated, also 1,4,5 and 7 while channel 6 is more or less isolated. Three dominating eigenvectors can be calculated from the covariances (Fig. 3.6). After orthogonal rotation using the Varimax criterion we can reveal 3 factors which determine 73% of the variances of all 7 TM channels over coastal waters. The strongest contribution to the common variances comes from channel 3, while channel 6 is nearly isolated (s. column H^2 in table 3.2). The factor loadings - which represent the correlation between the TM channels normalized radiances and the factors are also shown in Fig. 3.6. From these loadings and the correlation matrix we calculated the regression matrix in order to estimate the factor scores from the normalized image, which are the manifestations of the factors for each pixel.

The result is very surprising: factor 1 shows very clear the distribution of suspended matter (Fig. 3.7), while factor 2 independently maps the scattering of the atmosphere (Fig. 3.8). The image of factor 3 is very similar to the sea surface temperature distribution in channel 6, although it seems that also for this IR channel influences of the atmosphere are at least partly removed.

This example has demonstrated that it is possible to separate formal factors which independently determine the variation of the TM spectra and which can be related to real parameters as suspended matter, atmospheric scattering and SST. However, the application of this promising technique has to be further investigated within this project.

3.4 Radiative Transfer Model

The radiative transfer equation both for atmosphere and ocean is solved with the matrix-operator method. Although an azimuthally resolving version of this code is available, the small scanning angles of the Thematic Mapper of $\pm 5°$

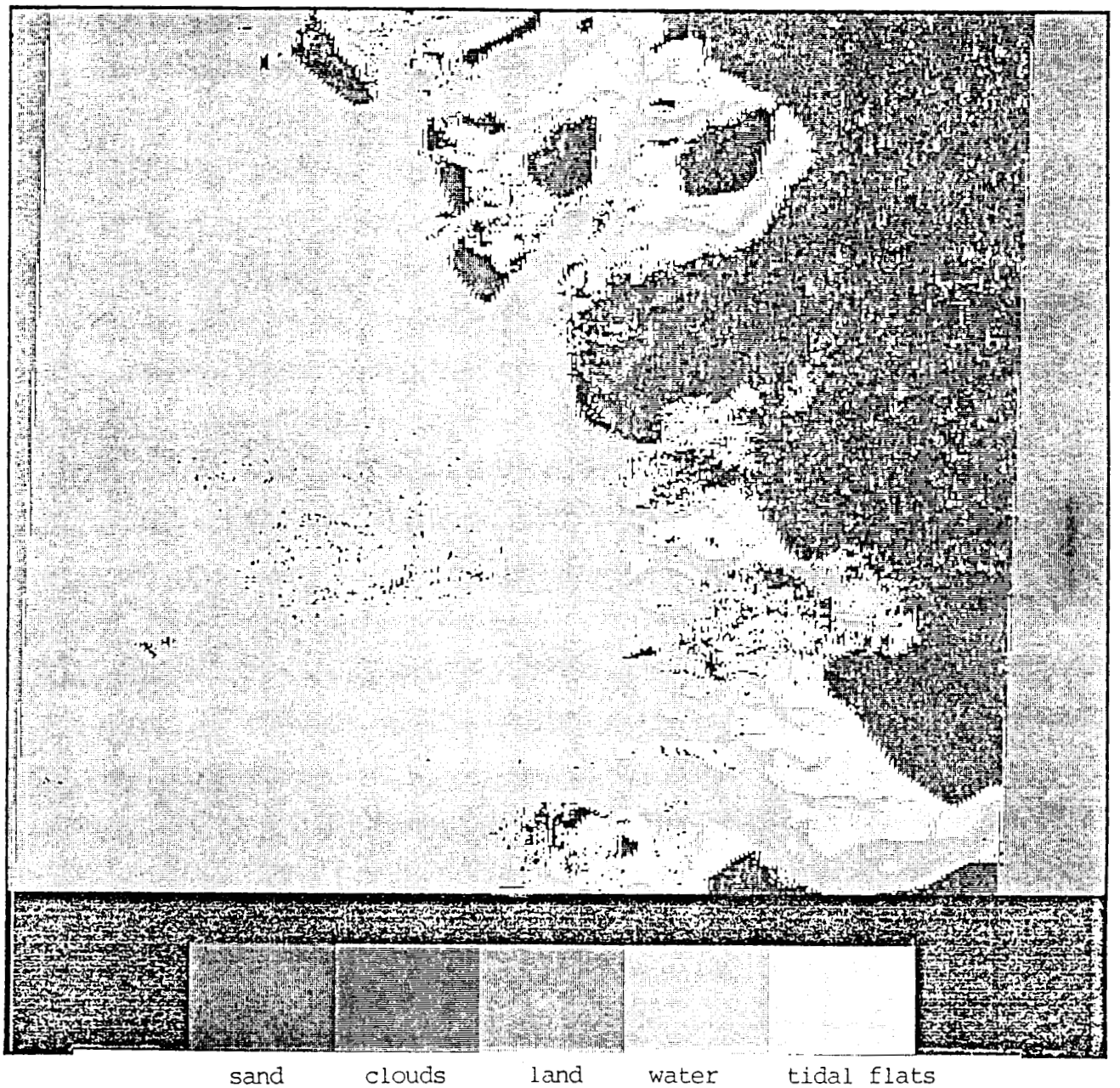

Figure 3.5: TM szene after classification to seperate the water area.

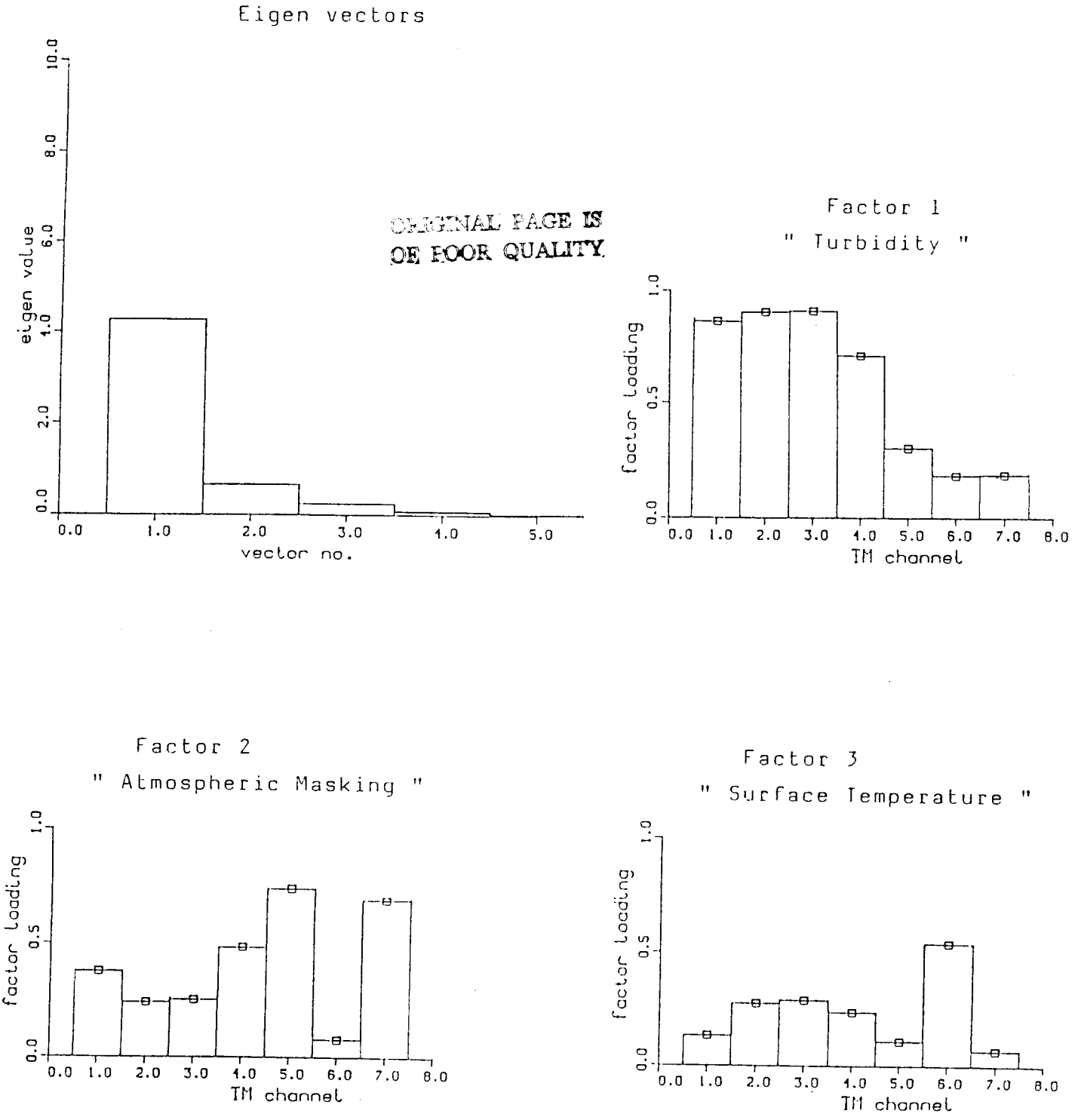

Figure 3.6: Eigenvalues and factor loadings for the "water area".

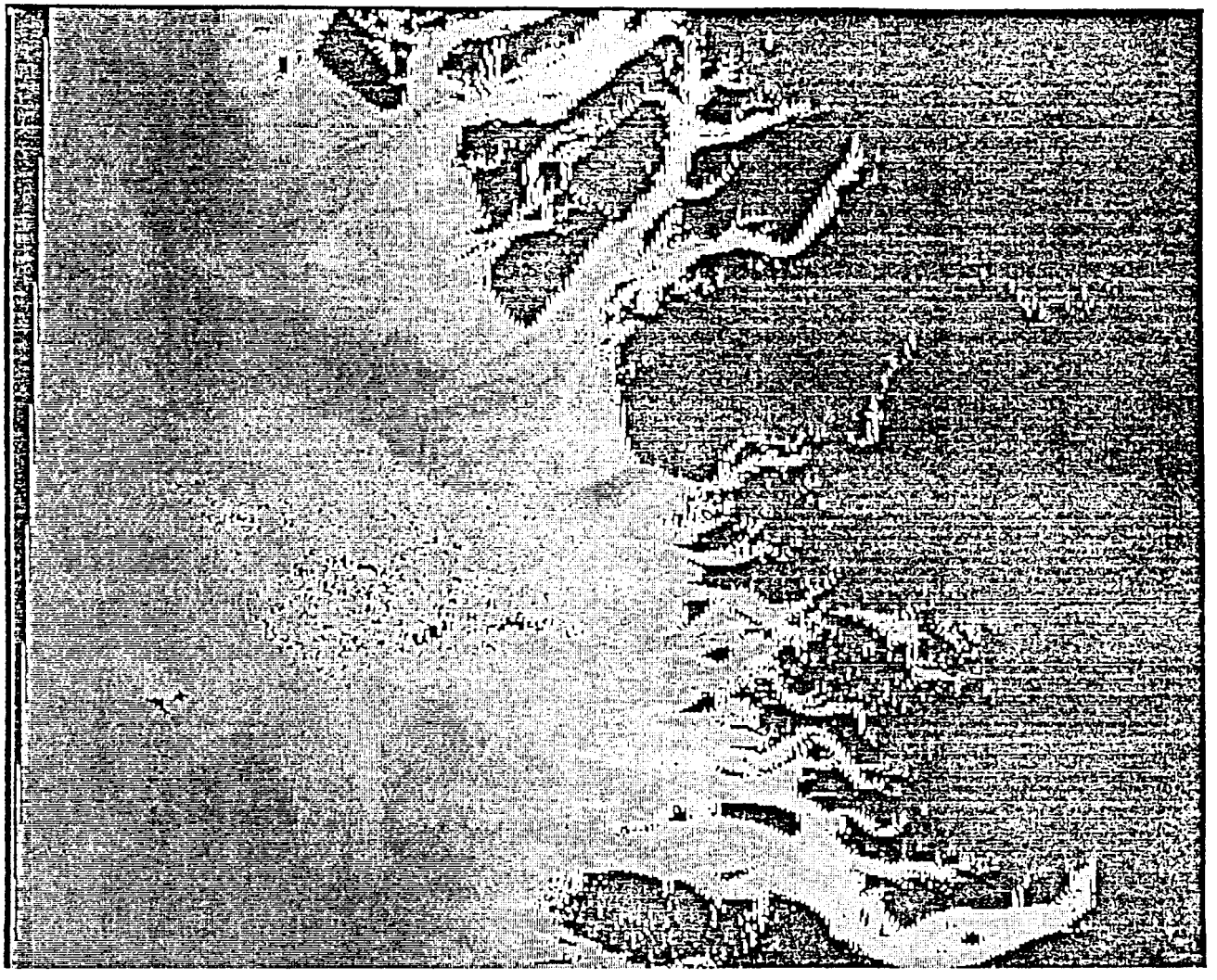

Figure 3.7: Image of scores for factor 1 indicationg the suspended matter distribution.

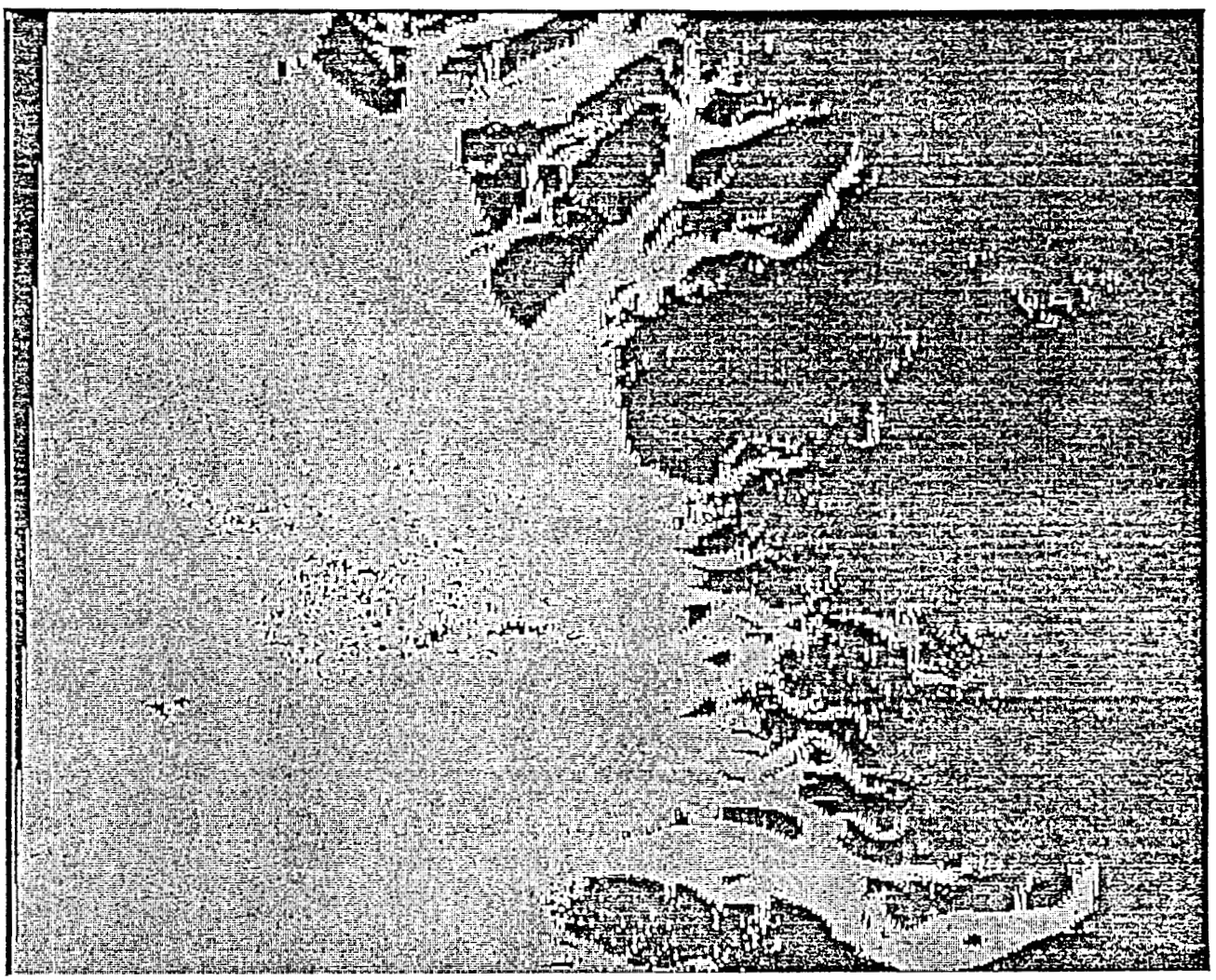

Figure 3.8: Image of scores for factor 2 indicating the atmosheric path radiance.

	F 1	F 2	F 3	H^2
TM 1	0.862	0.376	0.131	0.902
TM 2	0.904	0.241	0.276	0.951
TM 3	0.909	0.252	0.290	0.973
Tm 4	0.711	0.483	0.239	0.796
TM 5	0.302	0.745	0.110	0.658
TM 6	0.183	0.077	0.545	0.336
TM 7	0.187	0.692	0.070	0.159
VAR	3.051	1.536	0.548	5.136
%	43.583	21.947	7.834	73.364

Table 3.2: Rot. Factors and Kommunalitäten

around the nadir offers the choice of an azimuthally averaged code, which exactly determines nadir radiances. The rough ocean surface is handled as published in Fischer and Grassl (1984). The radiative transfer equation in the solar spectral range for a plane-parallel medium, is given by

$$\begin{aligned}(f\tfrac{d}{d\tau}+1)L(\tau,\mu',\phi,\lambda) = \; & \omega_0(\tau,\lambda)\cdot \\ & \cdot \int_0^{2\pi}\int_{-1}^{1} L(\tau,\mu',\phi',\lambda)\cdot P(\tau,\mu,\phi,\mu',\phi',\lambda)\, d\mu' d\phi' \\ & +\omega_0(\tau,\lambda)\,\pi\, F_0(\lambda)\, P(\tau,\mu,\phi,\mu_0,\phi_0,\lambda)\, e^{\frac{-\tau}{\mu_0}}\end{aligned} \tag{3.1}$$

The radiance L and the phase function P are both functions of height z, here expressed by the optical depth $\tau = \int_0^z c(z')dz'$, whereby the extinction coefficient $c = c^{(w)} + c^{(s)} + c^{(x)} + c^{(ys)}$ in coastal water is either the sum of pure water, phytoplankton, suspended matter, and yellow substance extinction in water or the sum of Rayleigh and Mie scattering in the atmosphere. L and P also depend on azimuth and zenith angle ϕ and θ ($\mu = cos\theta$) as well as on wavelength λ. The phase function P is a combination of all individual phase functions weighted with their respective scattering coefficients. The single scattering albedo ω_0 is the ratio of the total scattering and extinction coefficient. The solar spectral irradiance F_0 is taken from Neckel and Labs (1981).

Since the matrix operator method has been shown to give highly accurate solutions the main error sources in the solutions of Eq.(3.1) are improper optical parameters for given size distributions and compositions of distinct substance classes like suspended matter and phytoplankton.

An adequate simulation of Thematic Mapper measurements also requires an adaptation of the radiative transfer code to the characteristics of the TM channels (Barker,1981). Their poor spectral resolution does not resolve the changes of atmospheric and oceanic optical properties with respect to wavelength. As an

example, the transmission of water vapour, according to a midlatitude summer atmosphere, is shown in Fig. 3.9. Additionally, the transmission functions of the sensor filters have to be introduced (Markham and Barker, 1983). Therefore, we have to clarify, which spectral resolution for the radiative transfer code is necessary, in order to describe each of the TM channels.

For realistc variations of aerosol optical thickness between $\tau_a = 0.14$ and 0.77 at $\lambda = 550nm$, as well as of water substances in coastal areas we simulated the TM channels 1 - 5 with 1, 5, 10 and 20 nm spectral intervals. The calculations with 1 nm spectral resolution we accept as exact simulations. In table 3.3 the mean, maximum and minimum variations δ of upward radiances just below ocean surface and at the top of atmosphere due to the reduced spectral resolution of the radiation code are shown. The criterium chosen for a sufficient discription of the TM channels is that the errors are smaller than radiometric resolution (table 3.4). This is true for 10 nm resolution. Channel 5 may be simulated sufficiently accurate with 20 nm intervals.

3.5 Determination of Atmospheric Properties

A main problem in processing TM measurements is the determination of the multispectral water-leaving radiance by removing the atmospheric path radiance, which is primarily due to scattering by air molecules and aerosols and ocean surface reflection (Fig. 3.10). The accuracy of retrieved water substance concentrations is always limited by the accuracy of atmospheric correction.

The assumption of a single scattering process allows to seperate the measured radiance $L_{TM}(\lambda)$ of the TM into an ocean contribution $t(\lambda)L_w(\lambda)$, which is reduced by the diffuse transmission of the atmosphere $t(\lambda)$, and an atmospheric part due to scattering by aerosols $L_a(\lambda)$ and molecules $L_r(\lambda)$:

$$L_{TM}(\lambda) = t(\lambda)L_w(\lambda) + L_a(\lambda) + L_r(\lambda). \tag{3.2}$$

Following Gordon (1978,1981), the ocean leaving radiance $L_w(\lambda)$ at any wavelength λ may be calculated from satellite radiance $L_{TM}(\lambda_0)$, Rayleigh contribution $L_r(\lambda_0)$ and aerosol part $L_a(\lambda_0)$ at a near infrared wavelength λ_0 for which $L_w(\lambda_0) = 0$:

$$t(\lambda)L_w(\lambda) = L_{TM}(\lambda) - L_r(\lambda) - [S(\lambda, \lambda_0) \cdot (L_{TM}(\lambda_0) - L_r(\lambda_0))], \tag{3.3}$$

where $S(\lambda, \lambda_0) = [\tau_a(\lambda)F(\lambda)]/[\tau_a(\lambda_0)F(\lambda_0)]$ relates the optical thickness of the aerosols τ_a at different wavelengths and the spectral solar constant $F(\lambda)$. If we introduce $\tau_a(\lambda) \sim \lambda^{-\alpha}$, with the Ångstrøm-exponent α, we simply get

$$S(\lambda, \lambda_0) = \left(\frac{\lambda}{\lambda_0}\right)^{-\alpha} \left(\frac{F(\lambda)}{F(\lambda_0)}\right). \tag{3.4}$$

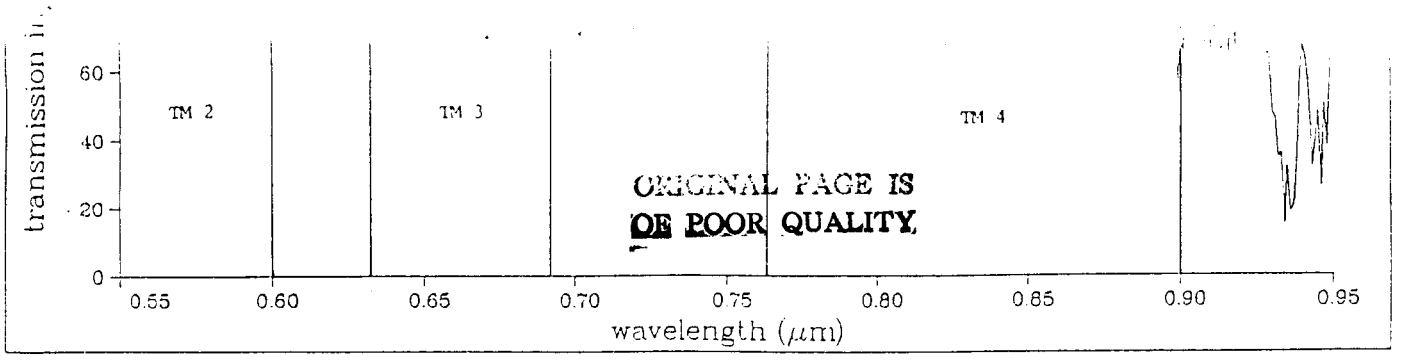

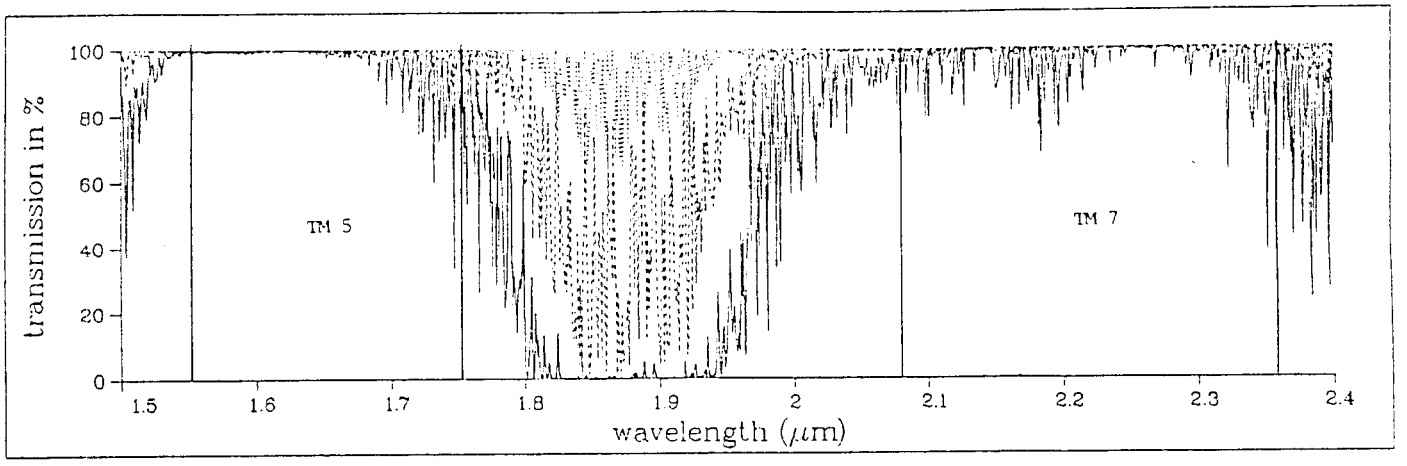

b)

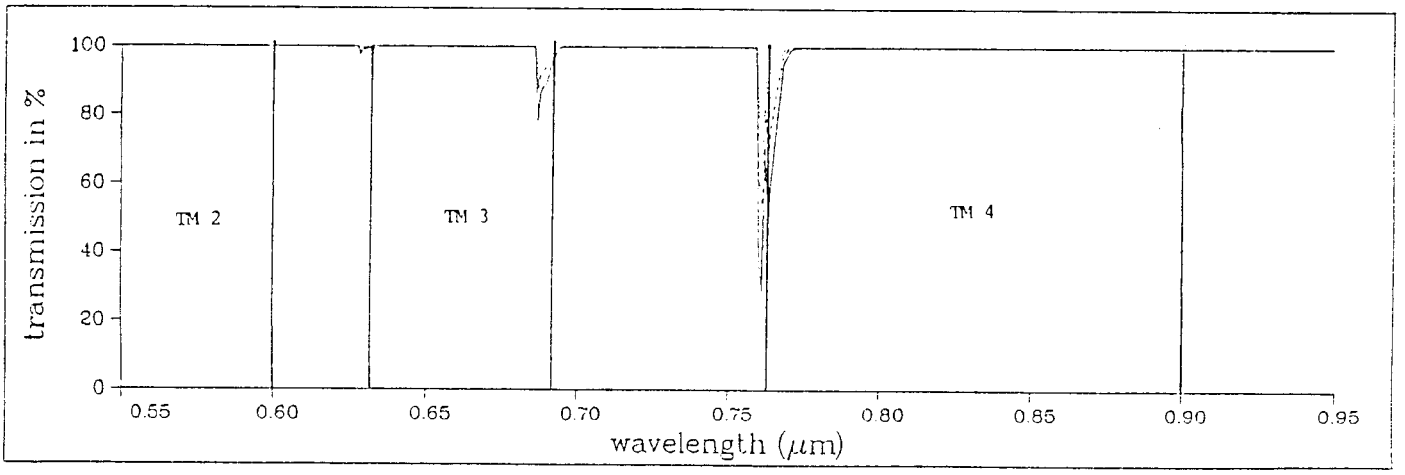

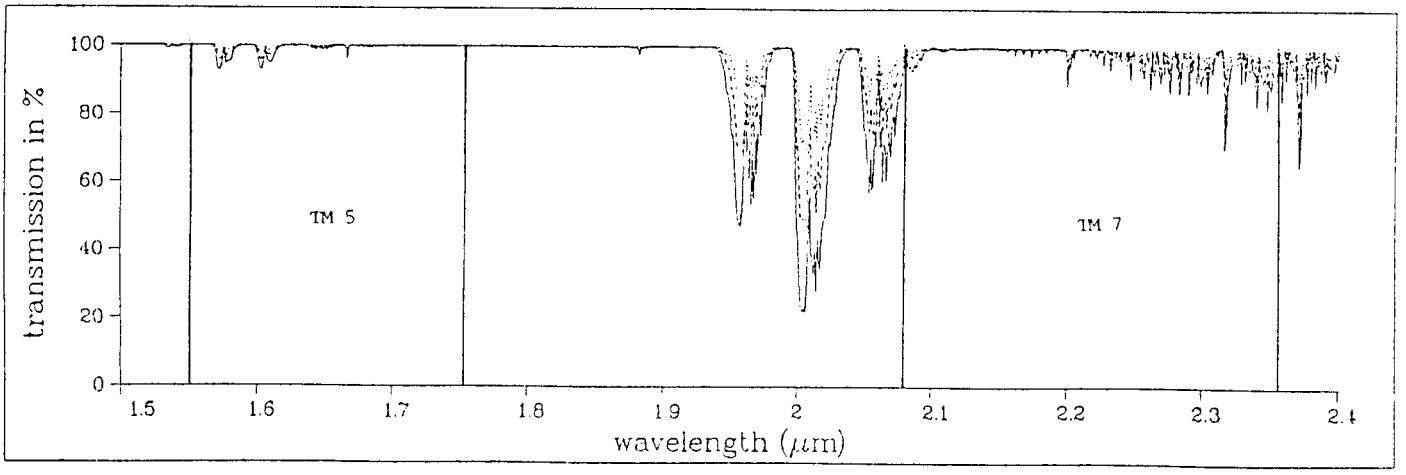

Figure 3.9: Transmittance of watervapour (a) and other atmospheric gases (O_2, O_3, CH_4 and other) (b), according to a midlatitude summer atmosphere.

a) spectral resolution: 5 nm

	TM1		TM2	
	z=-0.01	z=20000	z=-0.01	z=20000
δ	0.067	0.009	0.074	0.006
δ_max	0.387	0.70	0.430	0.045
δ_min	0.000	0.002	0.000	0.001

	TM3		TM4	
	z=-0.01	z=20000	z=-0.01	z=20000
δ	0.043	0.004	0.005	0.001
δ_max	0.246	0.026	0.027	0.008
δ_min	0.000	0.001	0.000	0.003

b) spectral resolution: 10 nm

	TM1		TM2	
	z=-0.001	z=20000	z=-0.001	z=20000
δ	0.222	0.014	0.245	0.009
δ_max	0.464	0.066	0.513	0.043
δ_min	0.000	0.003	0.000	0.002

	Tm3		TM4	
	z=-0.001	z=20000	z=-0.001	z=20000
δ	0.005	0.016	0.00	
δ_max	0.296	0.025	0.033	0.008
δ_min	0.000	0.001	0.000	0.003

c) spectral resolution: 20 nm

	TM1		TM2	
	z=-0.001	z=20000	z=-0.001	z=20000
δ	1.000	0.048	1.110	0.031
δ_max	1.116	0.156	1.280	0.100
δ_min	0.008	0.015	0.009	0.099

	Tm3		TM4	
	z=-0.001	z=20000	z=-0.001	z=20000
δ	0.639	0.018	0.071	0.006
δ_max	0.739	0.058	0.082	0.01
δ_min	0.005	0.006	0.000	0.002

Table 3.3: Mean δ, maximun δ_{max} and minimum δ_{min} radiance differences to the 1 nm resolution for different coarser resolutions. All readiances in $W/m^2 sr\mu m$:

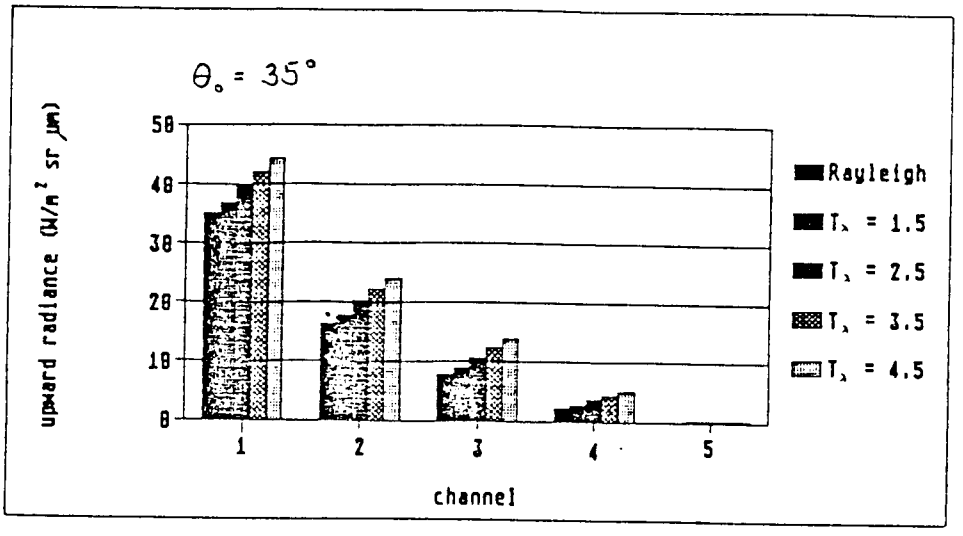

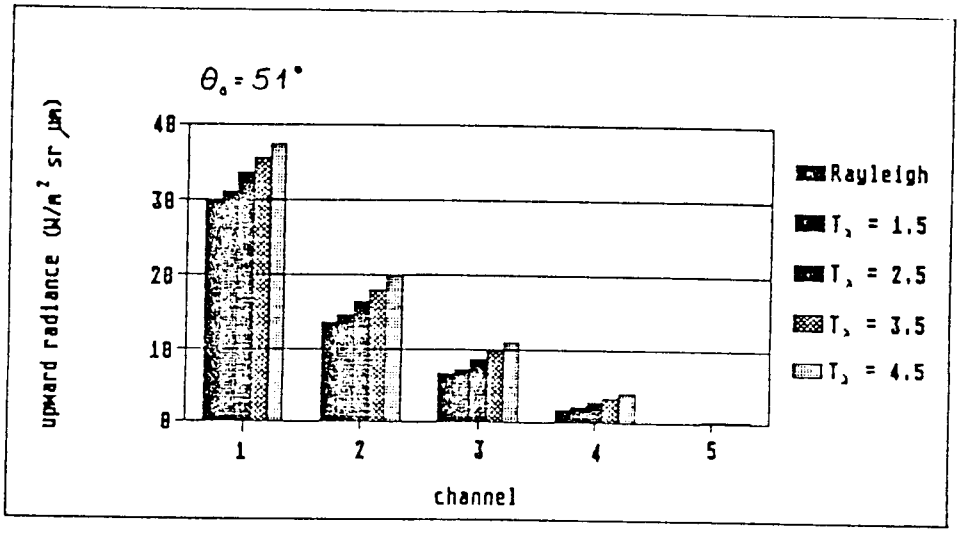

Figure 3.10: Upward radiances for TM channels 1-5 for a clear atmosphere and for various atmospheric turbidities - indicated by the Linke - turbidity factor.

TM1	TM2	TM3	TM4
0.596	1.71	0.808	0.329

Table 3.4: Radiometric resolution of the Thematic Mapper in $W/m^2 sr\mu m$ (referring to calibration values for 1 DN from 17th of May 1986).

As shown in Fig. 3.11 the power law for $\tau_a(\lambda) \sim \lambda^{-\alpha}$ is valid for the continental and maritime aerosols used in this study. The Ångstrøm-exponent can be determined from

$$\alpha = \frac{\ln \tau_a(\lambda_{01}) - \ln \tau_a(\lambda_{02})}{\ln \lambda_{02} - \ln \lambda_{01}}, \tag{3.5}$$

if the aerosol optical thickness τ_a at two wavelengths λ_{01} and λ_{02} is known.

To show the importance of knowing the Ångstrøm-exponent for atmospheric correction, the wavelength dependence of the extinction coefficients for maritime and continental aerosols are again given in Fig. 3.12, however, together with the TM channel intervals.

The Thematic Mapper channels 4 and 5 can in principle (see Fig. 3.13) be used for an estimation of aerosol type and concentration, as long as the concentration of suspended matter in water is low. As shown in Fig. 3.14 suspended matter concentration of more than 10 mg/l causes a non negligable contribution in channel 4, while channel 5 remains unaffected. In case of high concentrations we have to include the contribution of the ocean leaving radiance in channel 4 for a determination of the Ångstrøm exponent. The ratios of channel 4 and 5 show clearly differences for maritime and continental aerosols (Fig. 3.13). Fortunately this result is nearly independent on atmospheric turbidity and solar elevation.

However, the biggest problem is the poor radiometric resolution or low signal-to-noise ratio of the TM channels. The only way to overcome this restriction is an integrating over many pixels. Since we know from CZCS measurements that the horizontal distribution of aerosols is much more homogeneous than for water constituents, the lower spatial resolution is no drastic drawback. In order to analyze possible errors of the atmospheric correction we considered three different atmospheric conditions (table 3.5). If we assume a noise of ± 1 DN in channel 4 and 5, an increase of the number of integrated pixels reduces drastically the variations of channels 1-3, after subtraction of atmospheric path radiance. An integration of channel 4 and 5 by 33 $\times$ 33 pixels - nearly the pixel size of CZCS - further improves the atmospheric correction (see 3.5). The resulting maximum variation of $0.14 W/m^2 sr\mu m$ in channel 2 approximately corresponds - according to Fig. 3.14 - to a change of 0.25 mg/l suspended matter concentration.

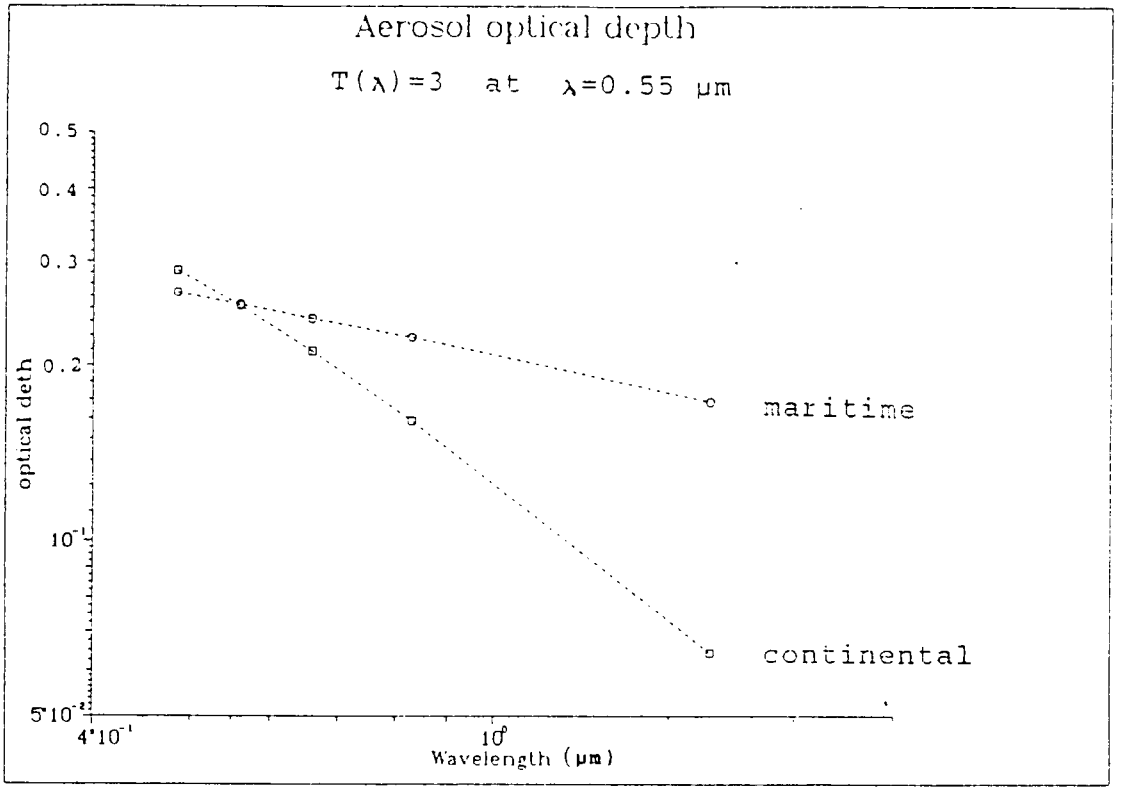

Figure 3.11: Aerosol optical depth due to continental or maritime aerosols as a function of wavelength.

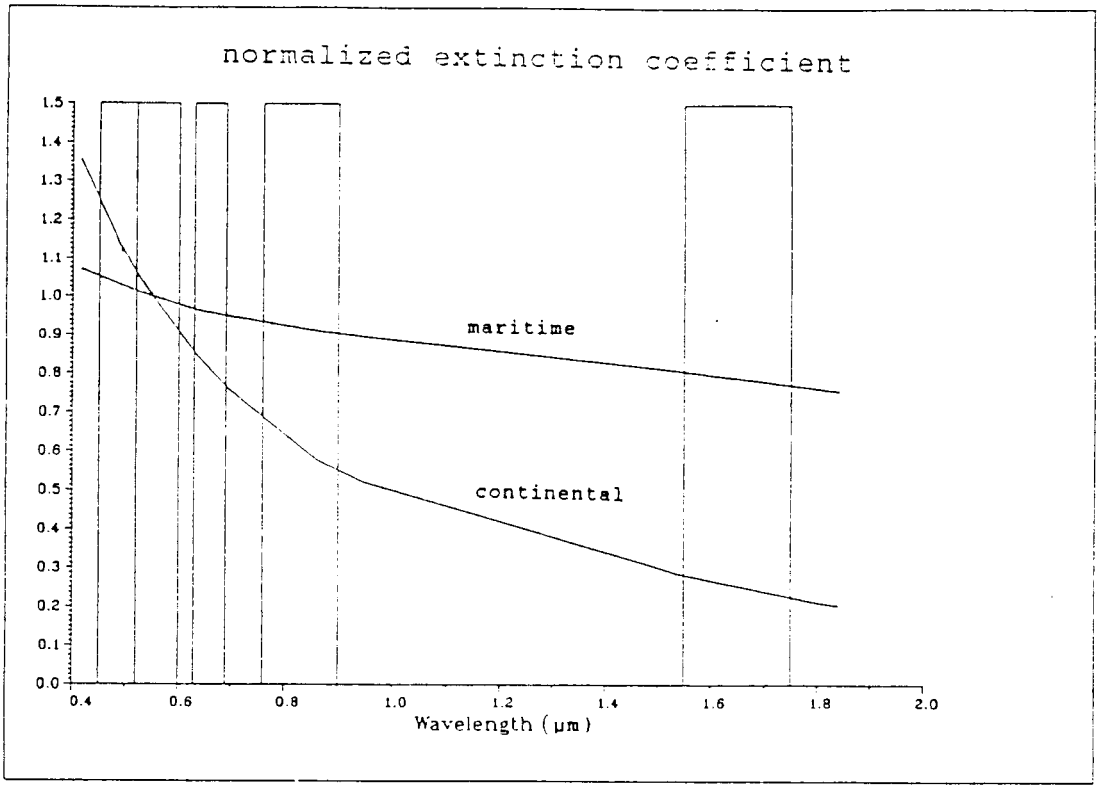

Figure 3.12: Normalized extinction coefficients for maritime and continental aerosols after Shettle and Fenn (1976); the TM channels are indicated.

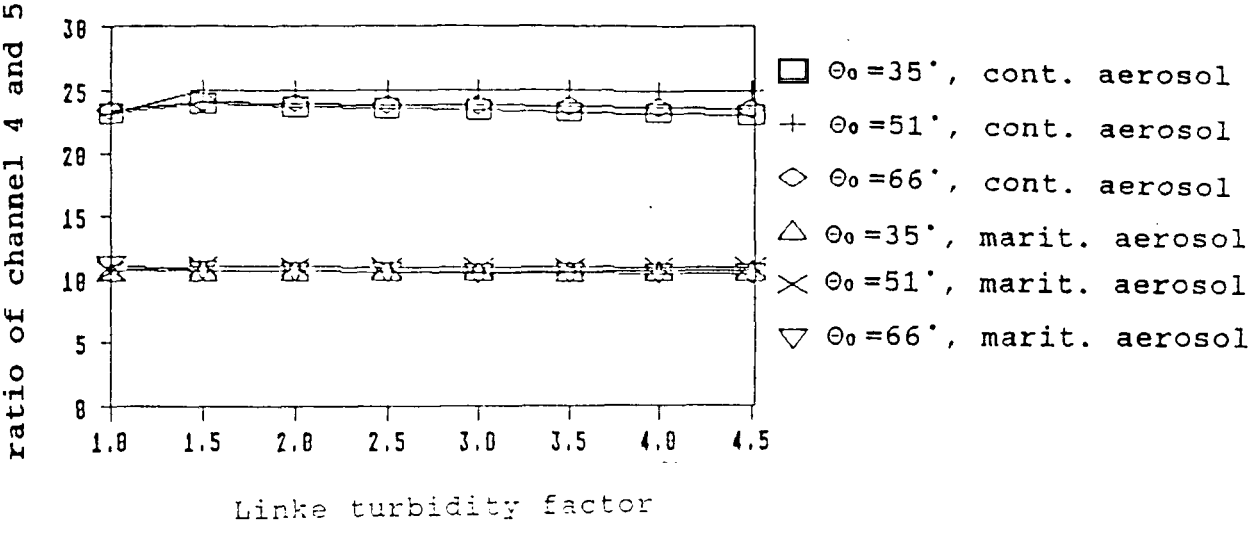

Figure 3.13: Radiance ratios of channels 4 and 5 depending on atmospheric turbidity; the contribution due to molecular scattering is substracted. The upper curves are for continental aerosols and the lower curves are for maritime aerosols; the different solar elevations are of minor importance for both types of aerosol.

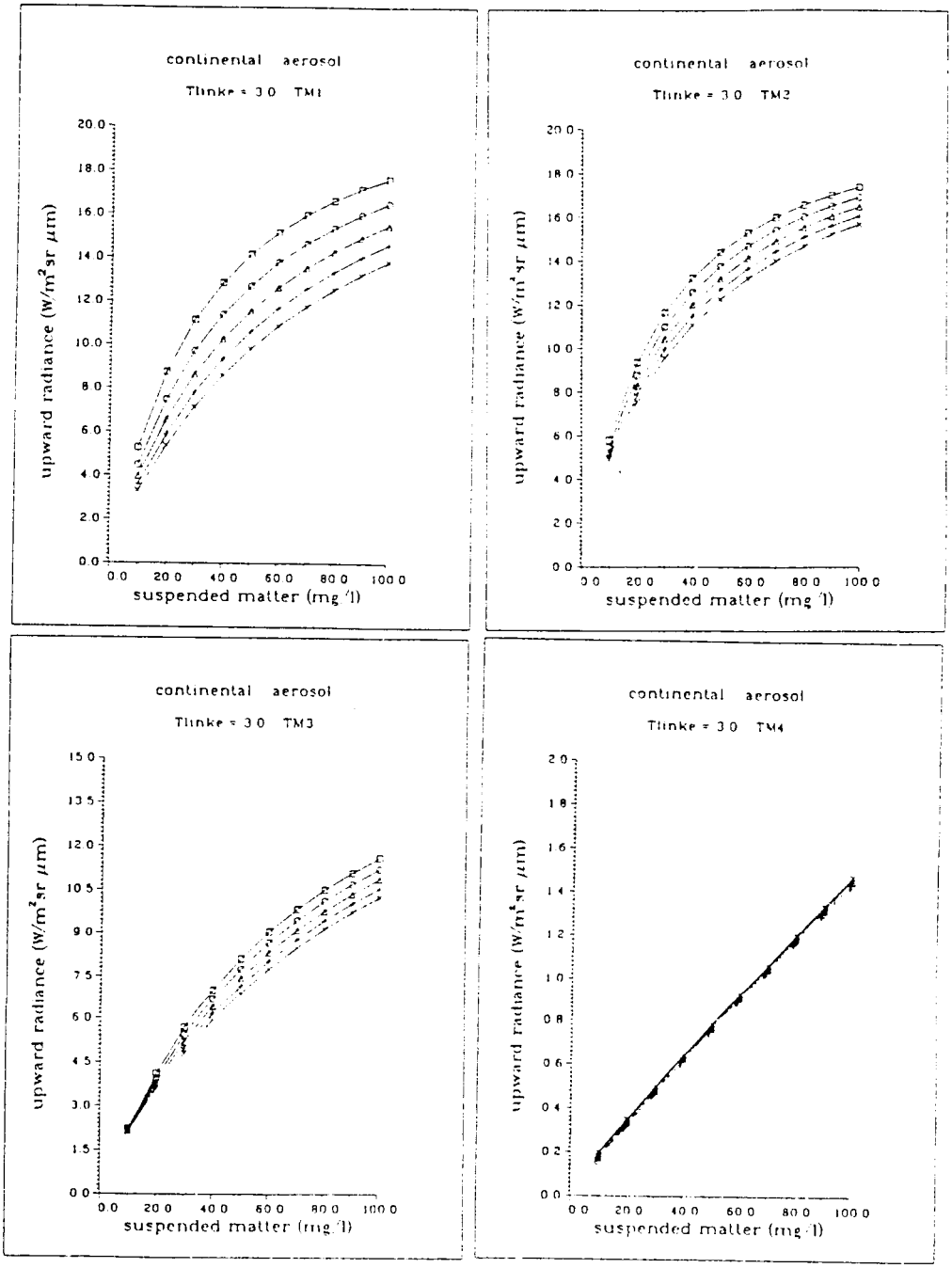

Figure 3.14: Upward radiances for TM channels 1-4 depending on suspended matter concentrations and for various chlorophyll concentrations : 0 $\mu g/l$ (□) , 5 $\mu g/l$ (○), 10 $\mu g/l$ (△) , 15 $\mu g/l$ (*) and 20 $\mu g/l$ (×) .The solar zenith angle is $\theta_0 = 50.7°$.

a)maritime aerosol , $\tau_a = 0.1$ at $\lambda = 550$ nm

n	1	3	5	9	11	33
TM1	3.63	1.05	0.61	0.33	0.27	0.09
TM2	2.76	0.83	0.48	0.26	0.22	0.07
TM3	1.75	0.55	0.32	0.18	0.15	0.05

b) maritime aerosol , $\tau_a = 0.3$ at $\lambda = 550$ nm

n	1	3	5	9	11	33
TM1	3.08	0.98	0.58	0.32	0.26	0.09
TM2	2.47	0.80	0.47	0.26	0.21	0.07
TM3	1.65	0.54	0.32	0.18	0.15	0.05

c) continental aerosol , $\tau_a = 0.3$ at $\lambda = 550$ nm

n	1	3	5	9	11	33
TM1	5.29	1.64	0.97	0.53	0.43	0.14
TM2	3.66	1.15	0.68	0.38	0.31	0.10
TM3	2.07	0.67	0.40	0.22	0.18	0.06

Table 3.5: Calculates errors of atmospheric radiance in $W/m^2 sr\mu m$ for channels 1, 2 and 3 caused by $\pm$ 1 DN in channels 4 and 5 depending on the number of pixels (n$\times$ n) over which is averaged:

3.6 Detection of Water Substances

A detection of water substances from Thematic Mapper measurements is only possible with channel 1, 2 and 3, because of the high absorption of water molecules at longer wavelengths. An evaluation of suspended matter in coastal waters is additionally restricted because of the low spectral resolution and the simultaneous occurance of phytoplankton and yellow substance.

A separation of water substances is difficult even for CZCS measurements, which are more suitable for water monitoring than TM measurements (Fischer et al., 1986). Whether the spectral resolution of the TM channels 1, 2 and 3 is sufficient for a separation is not clear up to now. However, the dominant water substance variations in coastal waters and estuaries are dominated by suspended matter. Phytoplankton and yellow substance reduce the upward radiances, mainly in channel 1 and less in channel 2 and 3, because of their absorption. We expect an underestimation of suspended matter concentration for areas with higher amounts of yellow substance and phytoplankton (Fischer et al., 1986). As shown in Fig. 3.14 an increase of chlorophyll from 0 to 20 $\mu g/l$ reduces the radiance in channel 2 by 1.9 and in channel 3 by $0.6 W/m^2 sr \mu m$ at a suspended matter concentration of 20 mg/l.

The low signal-to-noise ratio of the TM channels only allows a discrimination of roughly 2 mg/l per DN (see Table 2 and Fig. 3.14). If we assume a S/N ratio of 1 DN, only concenration classes of 5 mg/l can be detected. An avering over several pixels, i.e. 10×10 pixels, would enhence the the signal-to-noise ratio by a factor of 10. The resulting pixel size of $300 \times 300 m^2$ is still sufficient for most coastal water monitoring tasks, as shown in chapter 2.3.

For the development of a total suspended matter algorithm additional radiative transfer calculations will be performed, in order to set up a statistical basis, which allows us to validate concentrations retrieved from TM measurements.

Chapter 4

Conclusions

The factor analysis has shown that the suspended matter concentration, the atmsopheric scattering and the sea surface temperature can be retrieved as three independent factors, which determine the variation in the TM data over water areas. This method is also good for mapping the horizontal distribution of these parameters.

For the development of algorithms based on radiative transfer calculations it is necessary to elaborate an atmospheric correction procedure. The spectral channels in the near infrared (4 and 5) open the possiblity to determine the Ångstrøm exponent better than for the coastal zone colour scanner, if one integrates over about 30 × 30 pixels to improve the S/N ratio. The suspended matter distribution may then be calculated by the absolute radiance of channel 2 or 3 or the ratio of both.

Up to now we have no indication, whether the separation of chlorophyll is possible.

The distribution of suspended matter and sea surface temperature can be observed with the expected fine structure. Particularly the factor score image shows details, which have never been observed so far with other satellite data. At the present state we are optimistic in stating that the main task of our investigation concerning the suspended matter distribution will be reached with TM data.

The good correlation between water depth and suspended matter distribution as found from the ship data can now be analyzed for an entire area by the synoptic view of the TM scenes.

Chapter 5

Further effort

It is nearly impossible to compare the horizontal profiles recorded from the ship with the corresponding tracks in the image because even a time lag of only half an hour between TM data and the ship datacauses very marked changes in the suspended matter concentration at a location within this dynamic area. Thus a calibration of TM data is not possible by a direct comparison.

In order to link concentration data measured from the ship to the radiances of TM, we have to analyze the radiance spectra measured from board the ship and then apply the relation found to the TM scene after atmospheric correction. Another step will be a comparison with the Coastal Zone Colour Scanner scene for the same date.

The final investigation will concentrate on the analysis of scales using TM data, the ship profiles and bathymetric and current maps.

Bibliography

[1] J.L. BARKER, 1981: Relative Radiometric Calibration of Landsat TM Reflective Bands , Significant Figures for TM Dynamic Range Constants ;
in: Landsat-4 Science Characterisation , Early Results III - 145ff .

[2] R. DOERFFER, 1981: Factor Analysis in Ocean Color Interpretation;
in: Oceanography from Space, J.F.R.Gower, Ed. (Plenum Press, New York, 1981),pp.339-345.

[3] D. EISMA, 1981: Supply and deposition of suspended matter in the North Sea;
Spec. Publs. int. Ass. Sediment. 5, 415.

[4] J. FISCHER, 1984: Remote Sensing of Suspended Matter, Phytoplankton and Yellow Substances over Coastal Waters, Part 1: Aircraft Measurements;
Mitt. Geol.-Pal. Inst. Univ. Hamburg, SCOPE/UNEP Sonderbd. 55, 85.

[5] J. FISCHER & H. GRASSL, 1984: Radiative Transfer in an Atmosphere-Ocean System: An Azimuthally Dependent Matrix- Operator Approach;
Appl. Opt. 23, 1032.

[6] J. FISCHER, R. DOERFFER & H. GRASSL, 1986: Factor analysis of multispectral radiances over coastal and open ocean water based on radiative transfer calculations;
Appl. Opt. 25, 448-456.

[7] H.R. GORDON, 1978: Removal of atmospheric effects from satellite imagery of the oceans;
Appl. Optics 17, 1631.

[8] H.R. GORDON, 1981: A preliminary assessment of the Nimbus-7 CZCS atmospheric correction algorithm in a horizontal inhomogeneous atmosphere ;
in: Oceanography from Space, J.R.Gower, Ed., Plenum Press, New York, 257-266.

[9] B.L. MARKHAM & J.L. BARKER, 1983: Spectral characterization of the Landsat Thematic Mapper Sensors;
in: Landsat-4 Science Characterization, Early Results, Vol.II 235-276.

[10] H. NECKEL & D. LABS, 1981: Improved Data of Solar Spectral Irradiance from 330 to 1250 nm;
Sol. Phys. 74, 231.

[11] E.P. Shettle & R.W. Fenn, 1976: Models of the Atmospheric Aerosols and their Optical Properties;
ADARD Conf. Proc. 183.